haematologica
Journal of the Ferrata Storti Foundation

Interplay between circulating von Willebrand factor and neutrophils: implications for inflammation, neutrophil function, and von Willebrand factor clearance

by Alua Kuanyshbek, Hamideh Yadegari, Jens Müller, Nasim Shahidi Hamedani, Samhitha Urs Ramaraje, and Johannes Oldenburg

Received: January 2, 2024.
Accepted: December 23, 2024.

Citation: Alua Kuanyshbek, Hamideh Yadegari, Jens Müller, Nasim Shahidi Hamedani, Samhitha Urs Ramaraje, and Johannes Oldenburg. Interplay between circulating von Willebrand factor and neutrophils: implications for inflammation, neutrophil function, and von Willebrand factor clearance.
Haematologica. 2025 Jan 9. doi: 10.3324/haematol.2023.284919 [Epub ahead of print]

Interplay between circulating von Willebrand factor and neutrophils: implications for inflammation, neutrophil function, and von Willebrand factor clearance

Short title for the running head: Plasma VWF Interaction with Neutrophils

Alua Kuanyshbek,[1*] Hamideh Yadegari,[1*] Jens Müller,[1] Nasim Shahidi Hamedani,[1] Samhitha Urs Ramaraje,[1] and Johannes Oldenburg.[1]

[1]Institute of Experimental Haematology and Transfusion Medicine, University Hospital Bonn, Bonn, Germany

[*]A.K. and H.Y. contributed equally as co-first authors.

Corresponding author:
Dr. Hamideh Yadegari
Institute of Experimental Haematology and Transfusion Medicine
University Clinic Bonn
Venusberg-Campus 1
Germany
phone: +49 228 287 10532
fax: +49 228 287 14783
e-mail: hamideh.yadegari@ukbonn.de

Data sharing statement

For original data, please contact hamideh.yadegari@ukbonn.de

Acknowledgments

This work was supported by Bonfor SciMed research funding given to J.O. and H.Y.

Authors' Contribution: A.K. performed the experimental work and wrote the paper; H.Y. designed the study, supervised the study, interpreted the data, and wrote the paper; J.M. evaluated and interpreted flow cytometry data and edited the manuscript; N.SH. and SU.R contributed with VWF purification and edited the manuscript; and J.O. provided advice, evaluated data, reviewed and edited the manuscript.

Authors' Disclosures: The authors declare no conflicts of interest or financial disclosures related to this work.

Abstract

Von Willebrand factor (VWF) plays a critical role in hemostasis, and emerging evidence suggests its involvement in inflammation. Our study aimed to investigate the interaction between circulating plasma VWF and neutrophils (polymorphonuclear cells, PMNs), elucidate the fate of VWF after binding, and explore its impact on neutrophil behavior. Neutrophils were isolated from the whole blood of healthy volunteers, and their interaction with plasma VWF was examined ex vivo. Immunofluorescence imaging revealed an enhanced binding of VWF to neutrophils following stimulation with inflammatory agents (PMA, TNFα, and IL-8) and exposure to shear forces, highlighting a previously unknown interaction. Furthermore, immunofluorescence images demonstrated increased co-localization of VWF with the early endosome marker EEA1 and the late endosome marker Rab7 over time, indicating the uptake of VWF by neutrophils subsequent to the binding. This was supported by a significant decrease in VWF antigen levels in the supernatant of cells after stimulation. Moreover, stimulated neutrophils exposed to purified plasma-derived VWF exhibited elevated expression of neutrophil surface markers CD45 and CD66b, indicative of altered neutrophil function related to cell adhesion, migration, and phagocytosis. These findings suggest that VWF binding can modulate neutrophil function, potentially influencing their role in immune responses and inflammation. In summary, our study provides novel insights into the complex interplay between VWF and neutrophils, shedding light on the multifaceted roles of VWF in inflammation. Importantly, we have identified neutrophils as potential cellular mediators involved in the clearance of VWF from circulation, introducing a novel mechanism for VWF removal.

Keywords: von Willebrand Factor, Neutrophils, Inflammation, VWF Clearance, Polymorphonuclear Cells, PMNs

Introduction

Von Willebrand factor (VWF), a large multimeric plasma glycoprotein, plays a crucial role in primary and secondary hemostasis, where it facilitates platelet adhesion and aggregation at the site of vascular injury and stabilizes coagulation factor VIII (FVIII) in circulation.[1-4] However, beyond its established role in hemostasis, VWF has been found to play a multifaceted, complex role in inflammation that still needs further investigation.[5,6] Previous studies have suggested that VWF may modulate inflammation through both intracellular and extracellular pathways. Intracellularly, VWF has been shown to initiate the biogenesis of endothelial cell storage organelles called Weibel-Palade bodies (WPBs), which contain inflammatory mediators such as P-selectin, angiopoietin-2 (Ang2), interleukin 6 (IL-6), interleukin 8 (IL-8), and CXCL1.[7-9] This intrinsic ability of VWF to influence WPB formation suggests an indirect mechanism of inflammation modulation. Extracellularly, VWF, when immobilized or anchored to the endothelium, directly interacts with leukocytes, including polymorphonuclear leukocytes (PMNs, or known as neutrophils) and monocytes. The interaction of VWF with leukocytes involves binding to receptors such as P-selectin glycoprotein ligand-1 (PSGL-1) for rolling adhesion and Mac-1 (αMβ2 integrin [CD11b/CD18]) for stable adhesion.[10] Notably, the interaction between VWF and PMNs has been shown to enhance PMN recruitment and transmigration across the endothelium, thereby contributing to the initiation and propagation of inflammation.[6,11-13]

Furthermore, earlier in our laboratory, immunofluorescence (IF) staining of isolated neutrophils from healthy volunteers and from a patient with von Willebrand disease (VWD) (who exhibited an accelerated VWF clearance in plasma) surprisingly displayed VWF staining that was even stronger after the patient received therapeutic plasma-derived (pd)VWF concentrates. This observation suggested a potential interaction between unbound plasma (circulating) VWF and neutrophils.[14] Additional ex vivo investigations using endothelial colony-forming cells (ECFCs) derived from the VWD patient demonstrated malformed WPBs, impairing the recruitment of inflammatory cargoes and associated downstream signaling pathways. Transcriptome analysis revealed the overexpression of neutrophil-activating chemoattractants, including IL-6, IL-8, and CXCL-1, in patient-derived ECFCs compared to healthy volunteers.[14] These findings led us to propose that the overexpression of these chemoattractants could trigger neutrophil activation, increased binding of VWF to neutrophils, and consequent accelerated VWF uptake. Consequently, this previous study prompted the hypothesis that in addition to endothelium-anchored VWF, unbound (circulating) VWF might also interact with neutrophils, potentially contributing to VWF clearance from circulation, which forms the focus of our current investigation.

In this study, our objectives were to investigate the interaction of unbound plasma VWF with resting and stimulated neutrophils under both static and flow conditions. Additionally, we aimed to explore the internalization and fate of VWF following its interaction with human neutrophils by examining VWF trafficking within neutrophils. Furthermore, we sought to assess the effects of purified pdVWF/FVIII concentrate binding on the function and behavior of human neutrophils.

Methods

Isolation of human neutrophils

Whole blood (5-10 ml) was collected from healthy volunteers in EDTA tubes (Sarstedt, Germany) after obtaining informed consent, in compliance with the Declaration of Helsinki principles and the ethical guidelines of Germany. Neutrophils were isolated using the EasySep™ Direct Human Neutrophil Isolation Kit (StemCell Technologies, Germany). Cell number and viability were assessed with the NucleoCounter® NC-202™ (ChemoMetec, Denmark), and cell purity was confirmed by flow cytometry.

Flow cytometry

Neutrophils were washed in PBS, resuspended in staining buffer, and stained with fluorochrome-conjugated antibodies (anti-CD66b-FITC, anti-CD45-APC, anti-CD16-PE) or isotype controls (Miltenyi Biotec, Germany). Analysis was performed using a Navios EX Flow Cytometer (Beckman Coulter, Germany) and FlowJo software.

VWF binding to neutrophils upon activation

Neutrophils suspended in autologous plasma were either left untreated or stimulated with PMA (10 ng/ml), TNFα (5 ng/ml), or IL-8 (0.3-0.7 ng/ml) for 15 minutes at 37ºC. To test VWF binding via the Mac-1 receptor, neutrophils were treated with Neutrophil Inhibitory Factor (NIF; 400 ng/ml) for 30 minutes before PMA stimulation. VWF binding was assessed by IF microscopy.

VWF binding to neutrophils upon exposure to shear forces

Neutrophils were exposed to shear flow using the Bioflux 200 instrument (Fluxion Biosciences). Cells were resuspended in RPMI medium with pdVWF/FVIII (Haemate, CSL Behring, Germany) or recombinant VWF (VONVENDI®, Baxalta) and incubated under static or shear conditions (10 dyne/cm²) for 30 minutes at 37ºC. Cells were fixed and analyzed by IF microscopy.

VWF internalization and trafficking

VWF internalization was studied by co-localizing VWF with early (EEA1) and late (Rab7) endosomal markers using immunofluorescence microscopy. Neutrophils were fixed immediately or after 60 or 180 minutes of incubation. Additional experiments involved exposing neutrophils to shear stress, followed by incubation and subsequent IF analysis.

Immunofluorescence microscopy

Cells were fixed with formalin, permeabilized, and stained with primary antibodies against VWF, FVIII, CD11b, EEA1, and Rab7, followed by fluorescent secondary antibodies. Imaging was done with an Apotome.2 microscope (Carl Zeiss, Germany), and VWF signals and co-localization were quantified using ZEN 2.6 software.

Measurement of VWF content in supernatants

VWF levels in supernatants from resting and stimulated neutrophils were measured. After isolation, neutrophils were resuspended in autologous supernatant, stimulated with IL-8 (0.7 ng/ml), PMA (10 ng/ml), or TNFα (5 ng/ml) for 15 minutes at 37ºC, and VWF levels were compared with supernatants without cells.[15]

Purification of pdVWF/FVIII concentrates

The pdVWF/FVIII concentrate (Haemate) was purified by size-exclusion chromatography (ÄKTA pure 25 system, Cytiva) and protein purity was confirmed by SDS-PAGE.

Western blotting

Neutrophils were stimulated with IL-8 in the presence of autologous VWF, lysed, and subjected to western blotting using rabbit anti-human VWF antibodies.[16] Neutrophils, stimulated with IL-8 in the presence of FITC-labeled VWF (Invitrogen, USA), were lysed and analyzed by gel electrophoresis.

Effects of VWF on neutrophil characteristics

Neutrophils were stimulated with IL-8 or shear forces in the presence of pdVWF/FVIII and analyzed for surface proteins by flow cytometry. NETs (neutrophil extracellular traps) formation was assessed with and without pdVWF/FVIII.

Statistical analysis

Data significance was evaluated using the unpaired Student's t-test (GraphPad Prism 8.0.1). Results are presented as mean ± SEM, with $p \leq .05$ considered statistically significant.

Results

Highly viable and purified neutrophils were isolated from whole blood

The viability of isolated cells, determined by AO /DAPI on an automated cell counter, was between 99 to 100% for each isolation (Figure 1A-i). Flow cytometric analysis confirmed the purity of > 95% of the isolated neutrophils each time (Figure 1B). It was confirmed that > 95% of the isolated neutrophils were still viable after 180 min of incubation (Figure 1A-ii). In addition, > 90% of cells were nonapoptotic after 180 minutes, as determined by the level of CD16 shedding, a marker of neutrophil apoptosis (Figure 1C).

Neutrophils showed enhanced interaction with plasma VWF upon activation, ex vivo

IF images showed increased binding of plasma VWF to neutrophils after stimulation with the inflammatory modulators PMA, TNFα, and IL -8 and activation by shear forces, assessed by visual inspection and evaluation of VWF signal intensity (by measuring VWF MIV of at least 50 cells from three independent experiments). Cells stimulated with TNFα and PMA in the presence of autologous plasma VWF exhibited a significantly increased average MIV of VWF signal. The MIV values were 494.8 ± 23.9 and 517.3 ± 29.6, respectively, compared to 313 ± 10.9 in resting neutrophils (Figure 2A). Similarly, when neutrophils were treated with IL-8 concentrations of 0.3, 0.5, and 0.7 ng/ml, in the presence of autologous plasma VWF, there was a notable increase in VWF MIV. The respective MIV values were 534.4 ± 21.1, 700.4 ± 57.9, and 819.8 ± 58.4, compared to 313.5 ± 9.1 for untreated cells ($p \leq 0.0001$) (Figure 2B). Remarkably, the co-localization of VWF and CD11b, a constituent of the Mac-1 receptor, significantly intensified following the stimulation of neutrophils. This observation implies that VWF binds to the Mac-1 receptor upon interacting with neutrophils (Figure 2C). Further analysis, including NIF treatment, confirmed the binding of VWF to neutrophils through interaction with the Mac-1 receptor. NIF blocks the leukocyte Mac-1 (CD11b/CD18), inhibiting adhesion to its ligands. Our results demonstrated that neutrophils treated with NIF exhibited no detectable VWF signals and showed a significant reduction in CD11b signals. This confirms the effective inhibition of Mac-1 by NIF and its interference with VWF binding (Figure 2D).

Similarly, our results showed an increase in VWF MIV when neutrophils were exposed to shear flow (10 dyne/cm^2) in the presence of spiked pdVWF/FVIII, with a MIV of 443.3 ±

19.9 for shear-exposed cells versus a MIV of 297.5 ± 8.4 for unexposed cells (Figure 3A). Our supplemental experiments in which the isolated neutrophils were exposed to shear forces (10 dynes/cm^2) in the presence or absence of pdVWF/FVIII resulted in VWF MIV of 364.0 ± 25.3 and 256.2 ± 7.2, respectively (Figure 3B). This result confirmed that the increased VWF signal intensity was due to enhanced binding of the spiked pdVWF/FVIII and precluded possible synthesis of VWF by the neutrophils when exposed to shear forces. Similarly, we observed binding of rVWF when the neutrophils are exposed to shear force, demonstrated by an increase in VWF MIV in cells exposed to shear in presence of rVWF, compared with unexposed cells or absence of any VWF (Figure 3C). Furthermore, as anticipated, we detected the co-localization of VWF with factor VIII (Figure 3D).

Neutrophils internalize VWF after binding

IF images of neutrophils revealed that co-localization of VWF with the early endosome marker EEA1 and the late endosome Rab7 increased with incubation time, suggesting uptake of VWF into neutrophils after binding.

The IF image analysis of neutrophils isolated from whole blood and incubated directly for up to 180 min under static conditions showed that the Pearson coefficient of co-localization of VWF/EEA1 increased from 0.02 ± 0.01 at time 0 to 0.13 ± 0.01 after 60 min and to 0.24 ± 0.01 after 180 min ($p \leq 0.0001$) (Figure 4A). Similarly, the Pearson coefficient of VWF/Rab7 increased from 0.14 ± 0.01 at time 0 to 0.24 ± 0.01 after 60 min and 0.27 ± 0.01 after 180 min ($p \leq 0.0001$) (Figure 4B).

Comparable results were obtained when neutrophils were first exposed to shear flow in the presence of pdVWF/FVIII concentrates for 30 min and then incubated for 30- or 60-min. Analysis of the Pearson co-localization coefficient of VWF and EEA1 showed an increase from 0.11 ± 0.01 at time 0 to 0.20 ± 0.02 and 0.27 ± 0.02 after 30 and 60 min, respectively ($p \leq 0.0001$) (Figure 4C). Similarly, the co-localization coefficient of VWF and Rab7 showed an increase from 0.13 ± 0.01 at time 0 to 0.15 ± 0.02 and 0.29 ± 0.02 after 30 and 60 min, respectively (Figure 4D).

Furthermore, we demonstrated that the VWF:Ag concentration in the plasma supernatant of IL -8 (0.7 ng/ml), TNFα (5 ng/ml), and PMA (10 ng/ml)-stimulated neutrophils was reduced by an average of 2.6%, 2%, and 2.4% (p-value ≤ 0.001), respectively compared to the supernatant of resting cells and the negative control (supernatant deprived of cells) (Figure 5A).

VWF was degraded after uptake by neutrophils

Western blotting of lysates of resting neutrophils and IL -8 (0.7 ng/ml)-stimulated neutrophils (both incubated for 0, 60, and 180 min) revealed degraded VWF fragments around 20 and 70 kDa in addition to the intact full-length VWF (250 kDa). The strength of the bands corresponding to VWF degradation was more pronounced in stimulated cells (relative to intact VWF) than in resting cells (Figure 5B). Stimulation of neutrophils with IL -8 (0.7 ng/ml) in the presence of fluorescently labeled purified pdVWF/FVIII and subsequent gel electrophoresis yielded VWF fragments of the same size. This confirmed that VWF present in cell supernatants is internalized and degraded by neutrophils (Figure 5C).

VWF binding to neutrophils affects the surface expression of their functional proteins

We observed increased expression of CD45 and CD66b on the surface of neutrophils exposed to shear flow and cells stimulated with IL-8 in the presence of purified pdVWF/FVIII compared with cells without VWF in the cell suspension. The surface proteins CD45 and CD66b are essential markers of neutrophil function (cell adhesion, migration, and phagocytosis), and their expression levels may therefore be used to assess the activation and function of these cells.

Flow cytometric analysis showed a significant increase in the mean fluorescence intensity (MFI) average of CD66b and CD45 markers in shear-exposed neutrophils in the presence of VWF (an increased MFI of 35.3 ± 5.66% and 29.7 ± 7.37%, respectively) compared with those in the absence of VWF (p-value ≤0.001, and ≤0.01, respectively) (Figure 6A).

Similarly, we observed an increase in MFI average of 27.9 ± 10.12% and 15.2 ± 3.69%, respectively, for the surface proteins CD66b and CD45 on the surface of IL -8-stimulated cells in the presence of purified pdVWF/FVIII compared with those stimulated in the absence of VWF (p-value ≤ 0.05, and ≤0.01, respectively) (Figure 6B).

Moreover, we observed that VWF promotes the formation of NETs following the stimulation of isolated neutrophils with 25 ng/ml PMA, both in the presence and absence of VWF, across different incubation times of 60, 120, 180, and 240 minutes. According to the literature, NETosis occurs in distinct stages: initially, neutrophils exhibit larger but still segmented nuclei (around 60 minutes); this is followed by the disintegration of nuclei and chromatin decondensation (120-180 minutes); the late stages of NETosis (180-240 minutes) are characterized by the presence of cloudy and shooting cells, indicating that neutrophils have fully expelled their DNA; and finally, cells undergo lysis (240 minutes), where everything appears degraded.[17-20] The most significant differences between cells stimulated in the presence of VWF and those in its absence were observed after 120 and 180 minutes.

After 120 minutes, cells stimulated in the presence of VWF showed a greater number of cells with disintegrated nuclei compared to those stimulated in the absence of VWF. Additionally, after 180 minutes, a greater proportion of cells stimulated in the presence of VWF entered the NETosis phase (about 50% of cells showing a cloudy appearance and 50% a shooting form) compared to those in the absence of VWF (Figure 7).

Discussion

While VWF is widely recognized as a critical component in hemostasis, emerging evidence highlights its multifaceted involvement in vascular inflammation.[2,5,21] One proposed function of VWF in inflammation is its ability to recruit leukocytes to the site of injury when it is anchored onto the endothelium as bound VWF.[6,10] Bound VWF onto endothelium acts as an adhesive molecule, directly binding to leukocyte receptors (Mac-1 and P-selectin), facilitating leukocyte adhesion and migration. VWF also indirectly promotes the release of pro-inflammatory mediators by activating platelets.[22] VWF also influences the release of inflammatory modulators by triggering the biogenesis of endothelial storage organelles (WPBs) that contain cytokines, chemokines, and adhesion molecules.[7,14,23-26]

In our current study, we gained new insights into VWF's involvement in inflammation by investigating the interaction between plasma VWF (unbound) and neutrophils. We observed that unbound VWF interacts with neutrophils, resulting in enhanced expression of functional neutrophil surface proteins that indicate cell activation. We also demonstrated that neutrophils could internalize and degrade plasma VWF, suggesting their contribution to its removal from circulation. To our knowledge, our study is the first to investigate the interaction between plasma VWF and neutrophils under flow conditions, as well as in the presence of inflammatory molecules such as PMA, TNFα, and IL-8. Our analysis provides evidence that VWF binds to neutrophils through the Mac-1 receptor. Our findings complemented the previous work by Pendu et al., who demonstrated the attachment of bound (onto endothelium) VWF to integrin receptors on the surface of PMNs. We extended these findings by showing that unbound plasma VWF can also bind to integrin receptors. The β2 integrins are exclusively expressed on the surface of leukocytes, including neutrophils.[27] β2 integrins, particularly αMβ2 (Mac-1, CD11b/CD18), are crucial in the innate immune response, mediating interactions with endothelium, phagocytosis, degranulation, and cytokine production.[28-31] Integrins are typically found in an inactive state on the cell surface, but their activation occurs when agonists, such as chemokines or cytokines, bind to their receptors, triggering a switch to an active state.[28] Integrins exist as heterodimers, with the ability to adopt different conformations, each with distinct affinities for ligands: a low-affinity

bent conformation, an intermediate-affinity extended-closed conformation, and a high-affinity extended-open conformation .[32,33] Recent research suggests that multiple integrin conformations can coexist on the cell surface.[32] Additionally, mechanical forces exerted by blood flow can activate β2 integrins.[27] Our study revealed that a shear flow of 10 dynes/cm^2 resulted in the interaction between plasma VWF and neutrophils, and led to enhanced internalization. This shear flow value falls within the physiological range observed in arterial blood flow (10-20 dynes/cm^2).[34] These findings suggested that even under normal physiological conditions, plasma VWF can bind to and be internalized by neutrophils, potentially facilitated by shear flow-induced activation of β2 integrins. Furthermore, activating neutrophils with cytokines (e.g., IL8 and TNFα) enhanced the interaction between VWF and neutrophils, potentially further modulating this interaction.

Neutrophils employ multiple endocytosis mechanisms to internalize proteins, including clathrin-mediated endocytosis.[35-38] Our study specifically investigated the internalization of VWF by neutrophils using this mechanism. This process involves the binding of protein to cell surface receptors, internalization of the protein into clathrin-coated vesicles, the fusion of the vesicles with early endosomes (marked by EEA1) or late endosomes (marked by Rab7), as well as lysosomes, resulting in protein degradation. Our findings revealed an increasing co-localization of VWF with EEA1 and Rab7 over time, indicating the uptake of VWF by neutrophils, which was further enhanced under flow conditions. While our study focused on clathrin-mediated endocytosis, it is important to acknowledge that neutrophils may also utilize other endocytosis mechanisms for VWF internalization. Further, we confirmed the capability of neutrophils to uptake VWF by conducting experiments to assess VWF antigen levels in the supernatant of both resting and IL-8-stimulated neutrophils, as well as in supernatants without cells (used as a negative control). Significantly, we observed a decrease in VWF antigen levels in the supernatant of IL-8-activated neutrophils compared to the control groups. Furthermore, through protein analysis using western blotting, we demonstrated that VWF undergoes degradation upon binding to neutrophils. In this study, we observed VWF degradation products of 20 and 70 kDa, differing from the fragments produced by myeloid proteases as reported by Raife et al. .[39] The discrepancy between our VWF degradation products and those reported by Raife et al. may stem from different experimental setups and the cumulative effect of multiple proteases in our cell lysates. Raife et al. examined each enzyme separately, while our approach reflects an aggregated impact. Future proteomic analysis will help clarify these differences and determine the sequence of VWF fragments produced.

Survival of VWF in circulation is approximately 12 hours, but the mechanisms regulating VWF clearance from plasma are not fully elucidated. It is well-established that macrophages significantly contribute to VWF removal from circulation. Recent studies have identified various cell types and surface receptors involved in VWF clearance, including sinusoidal endothelial endocytic receptors stabilin-2 and CLEC4M, the hepatocyte receptor ASGPR, and macrophage receptors LRP1 and Siglec-5.[29,40-52] Our current study provides evidence for an additional novel cellular mechanism, highlighting the potential role of neutrophils in the clearance of plasma VWF. This mechanism, although likely one of several, underscores the multifaceted nature of VWF clearance processes. It remains to be elucidated whether neutrophils contribute to steady-state VWF clearance or primarily act during inflammatory responses to modulate VWF levels and mitigate thrombotic risk. Neutrophils' capacity to internalize and process proteins like albumin and fibrinogen during inflammation underlines their potential role in plasma homeostasis.[53,54] Further studies are needed to confirm their specific involvement in VWF clearance. The specific VWF domains or motifs responsible for the binding of circulating VWF to neutrophils are not yet understood. Identifying these domains is a key area for future research. Additionally, we speculate that VWF variants observed in VWD patients might influence the interaction between VWF and neutrophils, potentially affecting VWF uptake. Moreover, the impact of a complete absence of VWF (type 3 VWD) on neutrophil behavior and function remains unclear and warrants further investigation. In our study, we also observed that activated neutrophils, whether exposed to shear forces or stimulated with IL-8, exhibited increased expression of surface receptors CD45 and CD66b in the presence of VWF compared to when VWF was absent in the cell suspension. This finding suggests that VWF binding to neutrophils may modulate neutrophil receptor expression, possibly through the regulation of inside-out signaling pathways. To further elucidate the mechanisms by which VWF binding to neutrophils affects downstream signaling pathways, we are currently performing whole-transcriptome RNA-sequencing of neutrophils in our laboratory. This analysis will provide valuable insights into the alterations in gene expression and the underlying molecular mechanisms involved. CD45 and CD66b are receptors on neutrophils involved in immune cell activation, migration, adhesion, and effector functions.[55-59] Our study showing increased CD45 and CD66b expression on stimulated neutrophils in the presence of VWF suggests VWF's impact on neutrophil function and provided additional evidence for its role in inflammation. Furthermore, the current study demonstrated the impact of plasma VWF on promoting NETs formation.

Notably, a recent study found that VWF binding to macrophages triggers downstream MAP kinase signaling, NF-κB activation, and the production of pro-inflammatory cytokines and chemokines, thereby promoting monocyte chemotaxis. This study demonstrated a significant role for VWF in modulating macrophage function.[60]

Considering our results demonstrating the impact of VWF-neutrophil interaction on neutrophil behaviour, this may have implications in inflammatory diseases and the pathogenesis of thrombosis. Among the few studies reporting the impact of VWF on inflammation, Hillgruber et al. showed massive accumulation of VWF in skin biopsies of patients suffering from immune complex (IC)–mediated vasculitis (ICV). To clarify the impact of VWF on cutaneous inflammation, they induced experimental ICV in mice treated with VWF-blocking antibodies or in VWF-/- mice. Interference with VWF led to significant inhibition of the cutaneous inflammatory response, highlighting VWF's role incutaneous neutrophil recruitment. Anti-VWF treatment successfully blocked cutaneous inflammation. Similarly, further investigations are needed to assess the impact of VWF-neutrophil interaction on other pathological conditions such as thrombosis.

In conclusion, our study offers novel insights into the interplay between free circulating plasma VWF and neutrophils, shedding light on the impact of this interaction on neutrophil functions and highlighting the role of VWF in inflammation. Additionally, the findings of our study demonstrate the involvement of neutrophils in the clearance of VWF from circulation, suggesting their potential significance in enhancing therapeutic VWF concentrate preparations with an extended half-life for the effective treatment of patients with VWD.

References

1. Lyons SE, Ginsburg D. Molecular and cellular biology of von Willebrand factor. Trends Cardiovasc Med. 1994;4(1):34-39.
2. Luo G-P, Ni B, Yang X, Wu Y-Z. von Willebrand factor: more than a regulator of hemostasis and thrombosis. Acta Haematol. 2012;128(3):158-169.
3. Leebeek FWG, Eikenboom JCJ. Von Willebrand's Disease. N Engl J Med. 2016;375(21):2067-2080.
4. Schneppenheim R, Budde U. von Willebrand factor: The complex molecular genetics of a multidomain and multifunctional protein. J Thromb Haemost. 2011;9 Suppl 1:209-215.
5. Kawecki C, Lenting PJ, Denis CV. von Willebrand factor and inflammation. J Thromb Haemost. 2017;15(7):1285-1294.
6. Petri B, Broermann A, Li H, et al. von Willebrand factor promotes leukocyte extravasation. Blood. 2010;116(22):4712-4719.
7. McCormack JJ, Lopes da Silva M, Ferraro F, Patella F, Cutler DF. Weibel-Palade bodies at a glance. J Cell Sci. 2017;130(21):3611-3617.
8. Schillemans M, Karampini E, Kat M, Bierings R. Exocytosis of Weibel-Palade bodies: how to unpack a vascular emergency kit. J Thromb Haemost. 2019;17(1):6-18.
9. Valentijn KM, Sadler JE, Valentijn JA, Voorberg J, Eikenboom J. Functional architecture of Weibel-Palade bodies. Blood. 2011;117(19):5033-5043.
10. Pendu R, Terraube V, Christophe OD, et al. P-selectin glycoprotein ligand 1 and beta2-integrins cooperate in the adhesion of leukocytes to von Willebrand factor. Blood. 2006;108(12):3746-3752.
11. Koivunen E, Ranta TM, Annila A, et al. Inhibition of beta(2) integrin-mediated leukocyte cell adhesion by leucine-leucine-glycine motif-containing peptides. J Cell Biol. 2001;153(5):905-916.
12. Denis CV, Andre P, Saffaripour S, Wagner DD. Defect in regulated secretion of P-selectin affects leukocyte recruitment in von Willebrand factor-deficient mice. Proc Natl Acad Sci U S A. 2001;98(7):4072-4077.
13. Hillgruber C, Steingräber AK, Pöppelmann B, et al. Blocking von Willebrand factor for treatment of cutaneous inflammation. J Invest Dermatol. 2014;134(1):77-86.
14. Yadegari H, Jamil MA, Müller J, et al. Multifaceted pathomolecular mechanism of a VWF large deletion involved in the pathogenesis of severe VWD. Blood Adv. 2022;6(3):1038-1053.
15. Yadegari H, Driesen J, Pavlova A, Biswas A, Hertfelder H-J, Oldenburg J. Mutation distribution in the von Willebrand factor gene related to the different von Willebrand disease (VWD) types in a cohort of VWD patients. Thromb Haemost. 2012;108(4):662-671.
16. Yadegari H, Biswas A, Akhter MS, et al. Intron retention resulting from a silent mutation in the VWF gene that structurally influences the 5' splice site. Blood. 2016;128(17):2144-2152.
17. Inozemtsev V, Sergunova V, Vorobjeva N, et al. Stages of NETosis Development upon Stimulation of Neutrophils with Activators of Different Types. Int J Mol Sci. 2023;24(15):12355.
18. Brinkmann V, Reichard U, Goosmann C, et al. Neutrophil extracellular traps kill bacteria. Science. 2004;303(5663):1532-1535.
19. Fuchs TA, Abed U, Goosmann C, et al. Novel cell death program leads to neutrophil extracellular traps. J Cell Biol. 2007;176(2):231-241.
20. Papayannopoulos V, Metzler KD, Hakkim A, Zychlinsky A. Neutrophil elastase and myeloperoxidase regulate the formation of neutrophil extracellular traps. J Cell Biol. 2010;191(3):677-691.
21. Gragnano F, Sperlongano S, Golia E, et al. The Role of von Willebrand Factor in Vascular Inflammation: From Pathogenesis to Targeted Therapy. Mediators Inflamm. 2017;2017:5620314.

22. Koupenova M, Clancy L, Corkrey HA, Freedman JE. Circulating Platelets as Mediators of Immunity, Inflammation, and Thrombosis. Circ Res. 2018;122(2):337-351.
23. Nightingale TD, McCormack JJ, Grimes W, et al. Tuning the endothelial response: differential release of exocytic cargos from Weibel-Palade bodies. J Thromb Haemost. 2018;16(9):1873-1886.
24. Weibel ER, Palade GE. New cytoplasmic components in arterial endothelia. J Cell Biol. 1964;23(1):101-112.
25. Starke RD, Ferraro F, Paschalaki KE, et al. Endothelial von Willebrand factor regulates angiogenesis. Blood. 2011;117(3):1071-1080.
26. Yadegari H, Jamil MA, Marquardt N, Oldenburg J. A Homozygous Deep Intronic Variant Causes Von Willebrand Factor Deficiency and Lack of Endothelial-Specific Secretory Organelles, Weibel-Palade Bodies. Int J Mol Sci. 2022;23(6):3095.
27. Wen L, Moser M, Ley K. Molecular mechanisms of leukocyte β2 integrin activation. Blood. 2022;139(24):3480-3492.
28. Arnaout MA. Biology and structure of leukocyte β (2) integrins and their role in inflammation. F1000Res. 2016;5:F1000 Faculty Rev-2433.
29. O'Sullivan JM, Ward S, Lavin M, O'Donnell JS. von Willebrand factor clearance - biological mechanisms and clinical significance. Br J Haematol. 2018;183(2):185-195.
30. Fagerholm SC, Guenther C, Llort Asens M, Savinko T, Uotila LM. Beta2-Integrins and Interacting Proteins in Leukocyte Trafficking, Immune Suppression, and Immunodeficiency Disease. Front Immunol. 2019;10:254.
31. Podolnikova NP, Podolnikov AV, Haas TA, Lishko VK, Ugarova TP. Ligand recognition specificity of leukocyte integrin αMβ2 (Mac-1, CD11b/CD18) and its functional consequences. Biochemistry. 2015;54(6):1408-1420.
32. Bouti P, Webbers SDS, Fagerholm SC, et al. β2 Integrin Signaling Cascade in Neutrophils: More Than a Single Function. Front Immunol. 2020;11:619925.
33. Mezu-Ndubuisi OJ, Maheshwari A. The role of integrins in inflammation and angiogenesis. Pediatr Res. 2021;89(7):1619-1626.
34. Roux E, Bougaran P, Dufourcq P, Couffinhal T. Fluid Shear Stress Sensing by the Endothelial Layer. Front Physiol. 2020;11:861.
35. Swanson JA. Shaping cups into phagosomes and macropinosomes. Nat Rev Mol Cell Biol. 2008;9(8):639-649.
36. Borregaard N. Development of neutrophil granule diversity. Ann N Y Acad Sci. 1997;832:62-68.
37. Kerr MC, Teasdale RD. Defining macropinocytosis. Traffic. 2009;10(4):364-371.
38. Joshi B, Bastiani M, Strugnell SS, Boscher C, Parton RG, Nabi IR. Phosphocaveolin-1 is a mechanotransducer that induces caveola biogenesis via Egr1 transcriptional regulation. J Cell Biol. 2012;199(3):425-435.
39. Raife TJ, Cao W, Atkinson BS, et al. Leukocyte proteases cleave von Willebrand factor at or near the ADAMTS13 cleavage site. Blood. 2009;114(8):1666-1674.
40. O'Sullivan JM, Aguila S, McRae E, et al. N-linked glycan truncation causes enhanced clearance of plasma-derived von Willebrand factor. J Thromb Haemost. 2016;14(12):2446-2457.
41. van Schooten CJ, Shahbazi S, Groot E, et al. Macrophages contribute to the cellular uptake of von Willebrand factor and factor VIII in vivo. Blood. 2008;112(5):1704-1712.
42. Rawley O, O'Sullivan JM, Chion A, et al. von Willebrand factor arginine 1205 substitution results in accelerated macrophage-dependent clearance in vivo. J Thromb Haemost. 2015;13(5):821-826.
43. Rastegarlari G, Pegon JN, Casari C, et al. Macrophage LRP1 contributes to the clearance of von Willebrand factor. Blood. 2012;119(9):2126-2134.

44. Wohner N, Legendre P, Casari C, Christophe OD, Lenting PJ, Denis CV. Shear stress-independent binding of von Willebrand factor-type 2B mutants p.R1306Q & p.V1316M to LRP1 explains their increased clearance. J Thromb Haemost. 2015;13(5):815-820.
45. Rydz N, Swystun LL, Notley C, et al. The C-type lectin receptor CLEC4M binds, internalizes, and clears von Willebrand factor and contributes to the variation in plasma von Willebrand factor levels. Blood. 2013;121(26):5228-5237.
46. Sanders YV, van der Bom, J G, Isaacs A, et al. CLEC4M and STXBP5 gene variations contribute to von Willebrand factor level variation in von Willebrand disease. J Thromb Haemost. 2015;13(6):956-966.
47. Smith NL, Rice KM, Bovill EG, et al. Genetic variation associated with plasma von Willebrand factor levels and the risk of incident venous thrombosis. Blood. 2011;117(22):6007-6011.
48. Swystun LL, Lai JD, Notley C, et al. The endothelial cell receptor stabilin-2 regulates VWF-FVIII complex half-life and immunogenicity. J Clin Invest. 2018;128(9):4057-4073.
49. Manderstedt E, Lind-Halldén C, Lethagen S, Halldén C. Genetic variation in the C-type lectin receptor CLEC4M in type 1 von Willebrand Disease patients. PLoS One. 2018;13(2):e0192024.
50. Castro-Núñez L, Dienava-Verdoold I, Herczenik E, Mertens K, Meijer AB. Shear stress is required for the endocytic uptake of the factor VIII-von Willebrand factor complex by macrophages. J Thromb Haemost. 2012;10(9):1929-1937.
51. Chion A, O'Sullivan JM, Drakeford C, et al. N-linked glycans within the A2 domain of von Willebrand factor modulate macrophage-mediated clearance. Blood. 2016;128(15):1959-1968.
52. Atiq F, Rawley O, O'Sullivan JM, et al. R1205H (Vicenza) causes conformational changes in the von Willebrand factor D'D3 domains and enhances von Willebrand factor binding to clearance receptors LRP1 and SR-AI. J Thromb Haemost. 2024;22(10):2752-2760.
53. Becatti M, Emmi G, Silvestri E, et al. Neutrophil Activation Promotes Fibrinogen Oxidation and Thrombus Formation in Behçet Disease. Circulation. 2016;133(3):302-311.
54. Mantovani A, Cassatella MA, Costantini C, Jaillon S. Neutrophils in the activation and regulation of innate and adaptive immunity. Nat Rev Immunol. 2011;11(8):519-531.
55. Hermiston ML, Xu Z, Weiss A. CD45: a critical regulator of signaling thresholds in immune cells. Annu Rev Immunol. 2003;21:107-137.
56. Saunders AE, Johnson P. Modulation of immune cell signalling by the leukocyte common tyrosine phosphatase, CD45. Cell Signal. 2010;22(3):339-348.
57. Zhu JW, Doan K, Park J, et al. Receptor-like tyrosine phosphatases CD45 and CD148 have distinct functions in chemoattractant-mediated neutrophil migration and response to S. aureus. Immunity. 2011;35(5):757-769.
58. Gray-Owen SD, Blumberg RS. CEACAM1: contact-dependent control of immunity. Nat Rev Immunol. 2006;6(6):433-446.
59. Schröder AK, Uciechowski P, Fleischer D, Rink L. Crosslinking of CD66B on peripheral blood neutrophils mediates the release of interleukin-8 from intracellular storage. Hum Immunol. 2006;67(9):676-682.
60. Drakeford C, Aguila S, Roche F, et al. von Willebrand factor links primary hemostasis to innate immunity. Nat Commun. 2022;13(1):6320.

Legends

Figure 1. Viability verification and flow cytometry analysis of purified neutrophils from whole blood. Panel (A): Viability assessment of isolated neutrophils without incubation (W/O) or after 180 minutes (min) of incubation using the NucleoCounter® NC-202™. Viability was determined by acridine orange (AO) and DAPI staining for live and dead cells, respectively. **Panel (B):** Multicolor flow cytometry analysis confirming the purity of the cells (>95%). Neutrophils were analyzed directly after isolation using antibodies against specific surface receptors, including CD16, CD66b, and the leukocyte marker CD45, along with respective isotype controls. The gated CD45+ population demonstrated a typical neutrophil content (CD66b+CD16+) above 95%. The histograms depict neutrophils stained with anti-CD16-PE (red), anti-CD66b-FITC (green), and anti-CD45-APC (blue), incorporating isotype controls (gray). **Panel (C):** Assessment of apoptotic cells by evaluating CD16 receptor shedding after 180 min of incubation at 37ºC/5% CO_2 (ii), compared to cells analyzed immediately after isolation (W/O; i). The histograms display neutrophils stained with anti-CD16-PE (red), anti-CD66b-FITC (blue), and isotype controls (gray).

Figure 2. Analysis of VWF interaction with resting and activated neutrophils using immunofluorescence microscopy. Panel (A): Immunofluorescence microscopy images of unstimulated neutrophils (control, upper row) and neutrophils stimulated with TNFα (5 ng/ml) or PMA (10 ng/ml). The bar graph presents VWF MIV for unstimulated and stimulated neutrophils, which is calculated from at least 50 cells in three independent experiments. **Panel (B):** Immunofluorescence microscopy images of unsimulated neutrophils and neutrophils stimulated with different concentrations of IL-8 (0.3 ng/ml, 0.5 ng/ml, or 0.7 ng/ml). The bar graph demonstrates an increase in VWF MIVs with increasing IL-8 concentrations, quantified by VWF signals from at least 50 cells in three independent experiments. **Panel (C):** Co-localization coefficients of VWF and CD11b (a component of Mac-1 receptor [αMβ2 integrin]) determined from at least 25 regions of interest (25 cells) in three independent experiments. **Panel (D):** Immunofluorescence microscopy images of unstimulated neutrophils (control, upper row), neutrophils stimulated with PMA (10 ng/ml), as well as neutrophils stimulated with PMA (10 ng/ml) in presence of NIF (400 ng/ml). The bar graph presents VWF MIV for unstimulated and stimulated neutrophils, which is calculated from at least 50 cells in three independent experiments.

Immunofluorescence images show VWF (green), CD11b (red), and nucleus (DAPI, blue). The merge channel displays VWF-CD11b overlay. Scale bar: 10 µm. Statistical significance: ****: p≤0.0001, ***: p≤0.001, **: p≤0.01, *: p≤0.05.
VWF, von Willebrand factor; **rVWF**, recombinant VWF, **MIV**, mean intensity values; **NIF**, Neutrophil Inhibitory Factor

Figure 3. Investigating impact of shear flow on VWF interaction with neutrophils using immunofluorescence microscopy. Panel (A): Immunofluorescence images representing VWF binding to neutrophils exposed to shear flow (10 dyne/cm², lower row) compared to unexposed/resting cells (upper row). The bar graph shows measured VWF MIVs associated with unexposed and exposed neutrophils to shear flow, which was measured from at least 50 cells in three independent experiments. **Panel (B):** Immunofluorescence images of VWF staining in neutrophils exposed to shear flow in the presence and absence of pdVWF/FVIII. The bar graph illustrates VWF MIVs for exposed neutrophils with and without pdVWF/FVIII. Measurements were taken from at least 50 cells in three independent experiments for each condition. **Panel C:** Immunofluorescence images representing rVWF binding to neutrophils exposed to shear flow (10 dyne/cm², lower row) compared to unexposed/resting cells (upper row), as well as shear-exposed cells in absence of VWF (middle row). The bar graph shows measured VWF MIVs associated with unexposed and exposed neutrophils to shear flow, which was measured from at least 50 cells in three independent experiments. **Panel (D):** Immunofluorescence image demonstrating co-localization of VWF and factor VIII on neutrophils.
Immunofluorescence images show VWF (green), CD11b (red), and nucleus (DAPI, blue). The merge channel displays VWF-CD11b overlay. Scale bar: 10 µm. Statistical significance: ****: p≤0.0001, **: p≤0.01
VWF, von Willebrand factor; **rVWF**, recombinant VWF, **MIV**, mean intensity values

Figure 4. Intracellular trafficking of VWF after interaction with neutrophils in static and shear flow conditions. **Panels (A) and (B):** Immunostaining of neutrophils with VWF (green), EEA1 (early endosome marker, red in A), and Rab7 (late endosome marker, red in B) at different time points (0, 60, and 180 min) following their interaction with VWF under static conditions. Bar graphs show Pearson's co-localization coefficients of VWF/EEA1 and VWF/Rab7 over time, which was calculated from at least 25 cells of two independent experiments, each with three replicates (n=6). **Panels (C) and (D):** Immunostaining of neutrophils with VWF (green), EEA1 (red in C), and Rab7 (red in D) at different time points

(0, 30, and 60 min) following their interaction with VWF under flow conditions (10 dyne/cm^2 for 30 min). Bar graphs display Pearson's co-localization coefficients of VWF/EEA1 and VWF/Rab7 over time, which was measured from at least 50 cells of two independent experiments, each with three replicates (n=6)
Scale bar 10 µm. Statistical significance: ****: p≤0.0001, ***: p≤0.001, *: p≤0.05, ns (not significant): p>0.05
VWF, von Willebrand factor; **min/s**, minute/s

Figure 5. Evaluation of VWF quantity in neutrophil supernatant and VWF integrity in neutrophil lysates. Panel (A): Comparison of VWF:Ag levels in different supernatants to confirm VWF uptake by neutrophils. The left bar represents VWF:Ag value in supernatant without cells (negative control), set as 100%. The middle and right bars show mean values of VWF:Ag levels measured in supernatants of resting cells and cells stimulated with IL-8 (0.7 ng/ml), TNFα (5 ng/ml), and PMA (10 ng/ml) (n=6 for each), respectively. Statistical significance: ***: p≤0.001, ns (not significant): p>0.05. **Panel (B):** Western blot analysis of cell lysates, including resting neutrophils and IL-8 (0.7 ng/ml)-stimulated neutrophils (incubated for 0, 60, and 180 min), along with positive controls (lysate cells producing recombinant VWF, transfected HEK293T cells, and cells producing endogenous VWF, healthy ECFCs) and a negative control (mock HEK293T cells). Both resting and stimulated neutrophil lysates revealed degraded VWF fragments around 20 and 70 kDa in addition to intact full-length VWF (250 kDa). **Panel (C):** Gel electrophoresis of lysates from neutrophils stimulated with IL-8 (0.7 ng/ml) in the presence of fluorescently labeled purified VWF. Cells were lysed either immediately after stimulation with IL-8 in the presence of labeled VWF or incubated for an additional 60 or 180 min.
VWF, von Willebrand factor; **VWF:Ag**, VWF antigen; **ECFCs**, endothelial colony-forming cells; **min**, minutes, **IL-8**, interleukin-8

Figure 6. Effect of purified VWF on neutrophils by evaluating the expression of surface markers. Panel (A): Flow cytometry analysis demonstrates increased expression of surface markers CD66b (FITC) and CD45 (APC) on shear-exposed neutrophils in the presence of VWF compared to experiments without VWF. The histograms depict the expression levels of CD66b and CD45 on shear-exposed neutrophils isolated from five different healthy individuals (i-v) in the absence (light green) or presence of VWF (red), with isotype controls (grey) incorporated. The bar graph shows the CD66b and CD45 Mean Fluorescent Intensity (MFI) in neutrophils exposed to shear flow in the absence or pres-

ence of VWF, determined from five different experiments. **Panel (B):** Flow cytometry analysis shows increased expression of surface markers CD66b (FITC) and CD45 (APC) on IL-8-stimulated neutrophils in the presence of VWF compared to experiments without VWF. The histograms display the expression levels of CD66b and CD45 on stimulated neutrophils isolated from five different healthy individuals (i-v) in the absence (light blue) or presence of VWF (marine blue), incorporating isotype controls (grey). The bar graph shows the CD66b and CD45 MFI in neutrophils stimulated with IL-8 in the absence or presence of VWF, determined from five different experiments.
Statistical significance: ****: p≤0.0001, ***: p≤0.001, **: p≤0.01, *: p≤0.05.
VWF, von Willebrand factor; **MFI**, mean fluorescent intensity; **IL-8**, interleukin-8

Figure 7. Effect of pdVWF/FVIII concentrate on neutrophil extracellular traps (NETs). Isolated neutrophils were stimulated with 25 ng/ml PMA for 120 and 180 minutes, in the presence or absence of pdVWF/FVIII concentrate. The figure presents results for these time points, reflecting the late stages of NETosis. At 120 minutes, neutrophils exhibit disintegrated nuclei and chromatin decondensation. By 180 minutes, the cells show characteristic NETosis features, including cloudy and shooting cells, indicating complete expulsion of DNA. After stimulation, cells were fixed and subjected to immunofluorescence staining using CitH3 antibody, CD11b, and DAPI to visualize NET formation. Scale bar 20 µm.

Figure 1

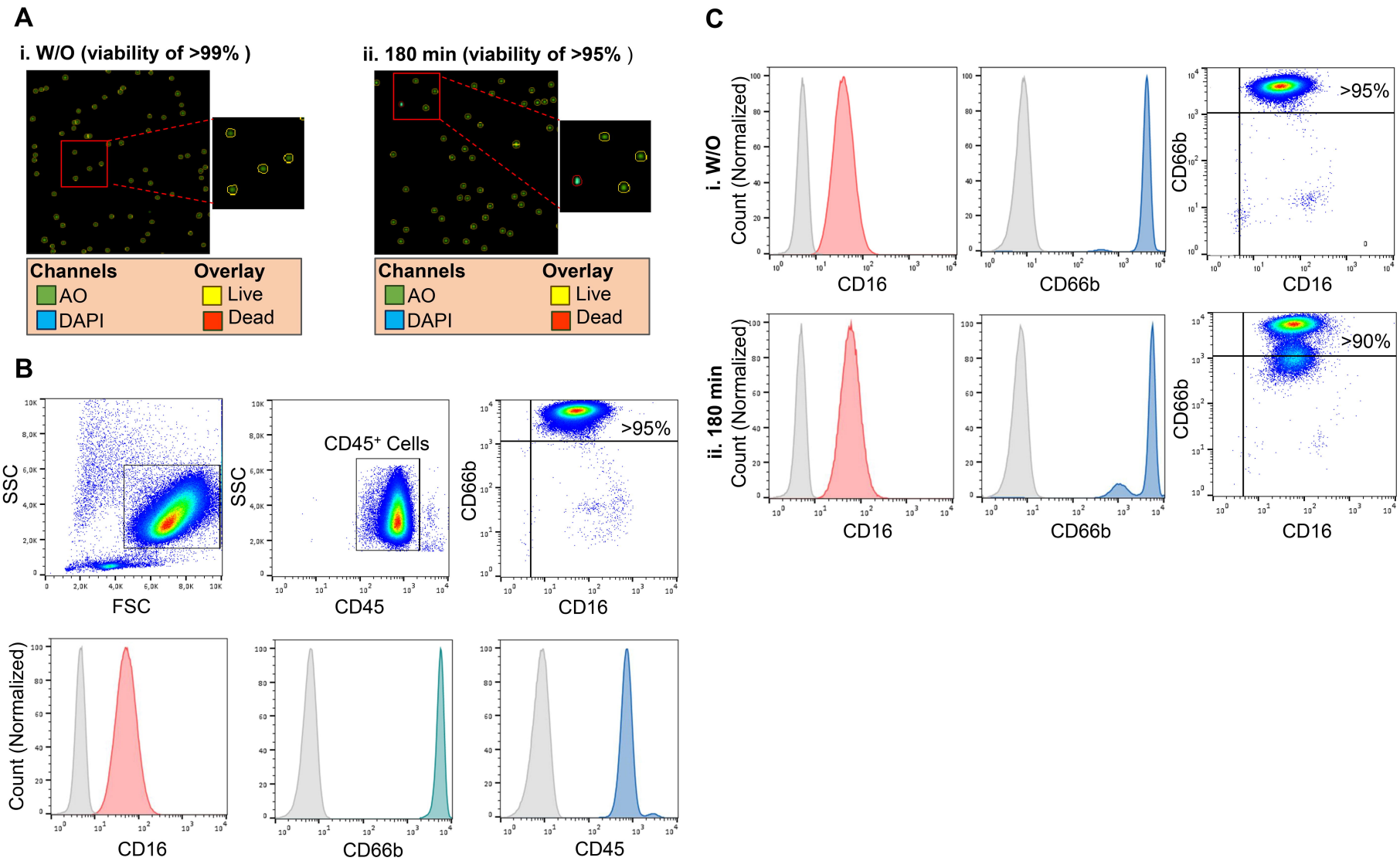
A
i. W/O (viability of >99%)
ii. 180 min (viability of >95%)
Channels
AO
DAPI
Overlay
Live
Dead
B
SSC
FSC
CD45⁺ Cells
CD45
CD66b
CD16
>95%
Count (Normalized)
C
i. W/O
ii. 180 min
>95%
>90%

Figure 2

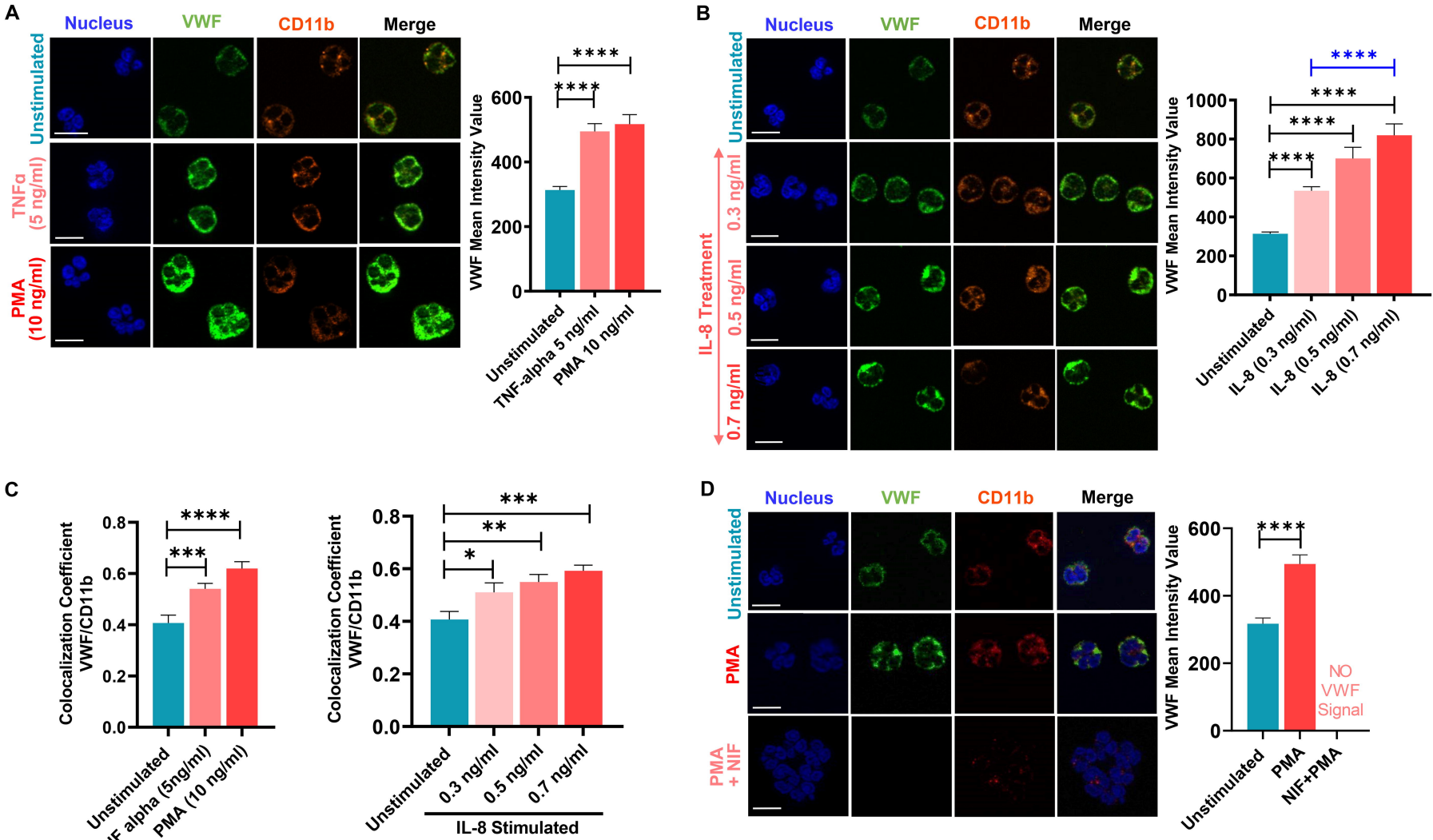
A
Nucleus
VWF
CD11b
Merge
Unstimulated
TNFα (5 ng/ml)
PMA (10 ng/ml)
VWF Mean Intensity Value
Unstimulated
TNF-alpha 5 ng/ml
PMA 10 ng/ml
B
IL-8 Treatment
0.3 ng/ml
0.5 ng/ml
0.7 ng/ml
Unstimulated
IL-8 (0.3 ng/ml)
IL-8 (0.5 ng/ml)
IL-8 (0.7 ng/ml)
C
Colocalization Coefficient VWF/CD11b
Unstimulated
TNF alpha (5ng/ml)
PMA (10 ng/ml)
IL-8 Stimulated
D
PMA + NIF
NO VWF Signal
NIF+PMA

Figure 3

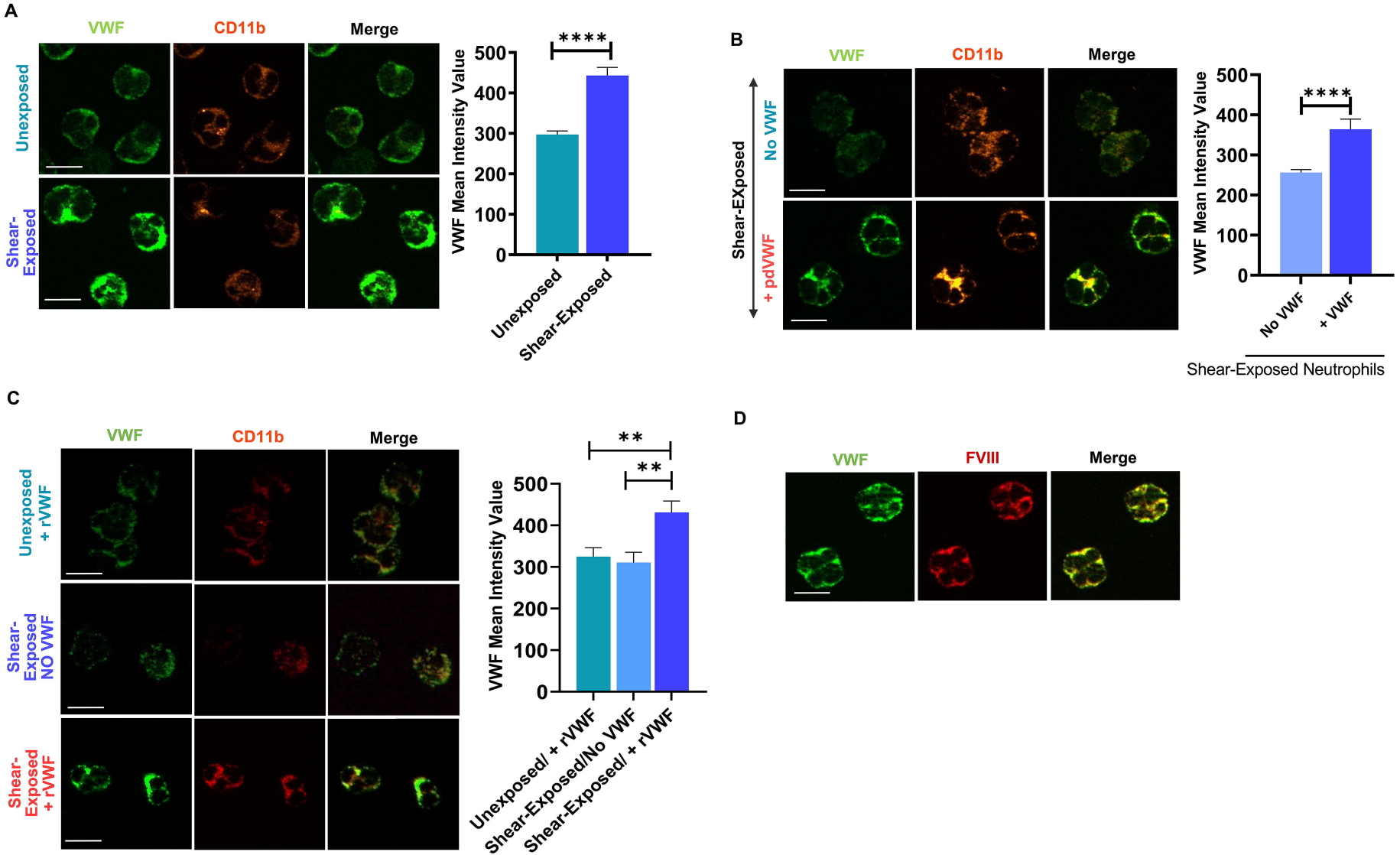
A
VWF
CD11b
Merge
Unexposed
Shear-Exposed
VWF Mean Intensity Value
500
400
300
200
100
0
****
Unexposed
Shear-Exposed
B
VWF
CD11b
Merge
Shear-EXposed
No VWF
+ pdVWF
VWF Mean Intensity Value
500
400
300
200
100
0
****
No VWF
+ VWF
Shear-Exposed Neutrophils
C
VWF
CD11b
Merge
Unexposed + rVWF
Shear-Exposed NO VWF
Shear-Exposed + rVWF
VWF Mean Intensity Value
500
400
300
200
100
0
**
**
Unexposed/ + rVWF
Shear-Exposed/No VWF
Shear-Exposed/ + rVWF
D
VWF
FVIII
Merge

Figure 4

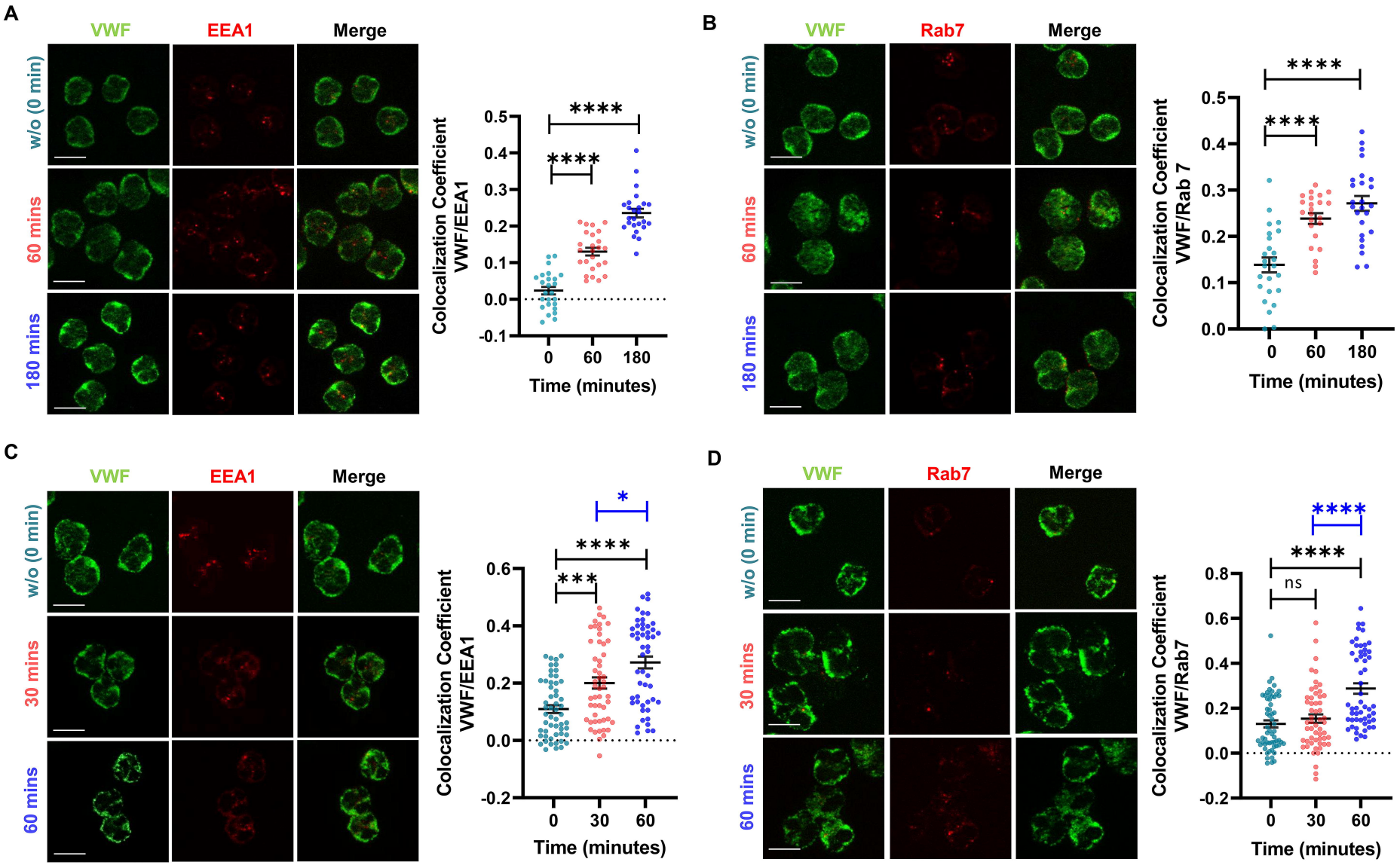
A
VWF
EEA1
Merge
w/o (0 min)
60 mins
180 mins
Colocalization Coefficient VWF/EEA1
****
****
0.5
0.4
0.3
0.2
0.1
0.0
-0.1
0
60
180
Time (minutes)
B
VWF
Rab7
Merge
w/o (0 min)
60 mins
180 mins
Colocalization Coefficient VWF/Rab 7
****
****
0.5
0.4
0.3
0.2
0.1
0.0
0
60
180
Time (minutes)
C
VWF
EEA1
Merge
w/o (0 min)
30 mins
60 mins
Colocalization Coefficient VWF/EEA1
*
****
***
0.6
0.4
0.2
0.0
-0.2
0
30
60
Time (minutes)
D
VWF
Rab7
Merge
w/o (0 min)
30 mins
60 mins
Colocalization Coefficient VWF/Rab7
****
****
ns
0.8
0.6
0.4
0.2
0.0
-0.2
0
30
60
Time (minutes)

Figure 5

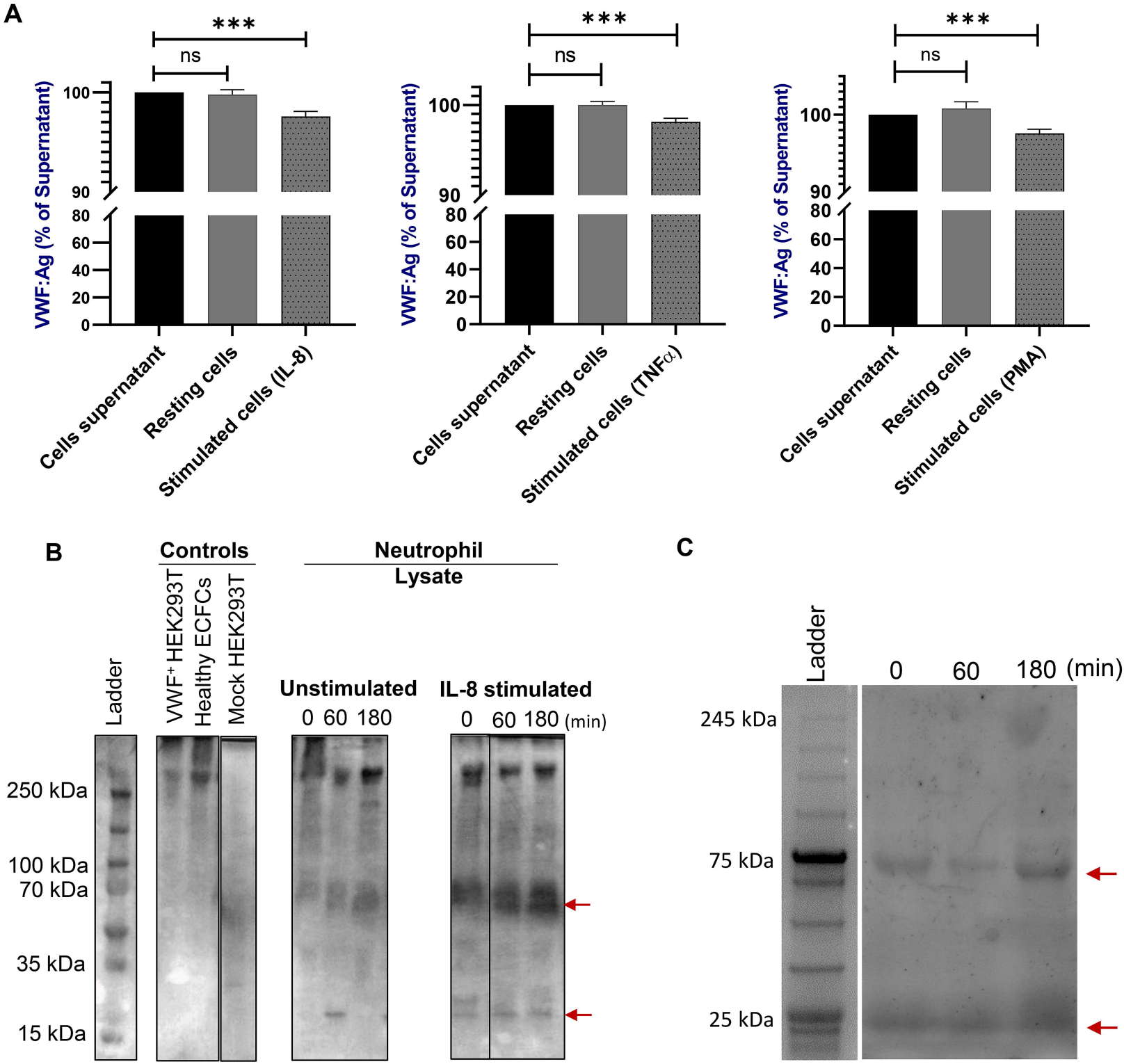
A
***
ns
VWF:Ag (% of Supernatant)
100
90
80
60
40
20
0
Cells supernatant
Resting cells
Stimulated cells (IL-8)
Stimulated cells (TNFα)
Stimulated cells (PMA)
B
Controls
Neutrophil Lysate
Ladder
VWF+ HEK293T
Healthy ECFCs
Mock HEK293T
Unstimulated
IL-8 stimulated
0 60 180 (min)
250 kDa
100 kDa
70 kDa
35 kDa
15 kDa
C
Ladder
0 60 180 (min)
245 kDa
75 kDa
25 kDa

Figure 6

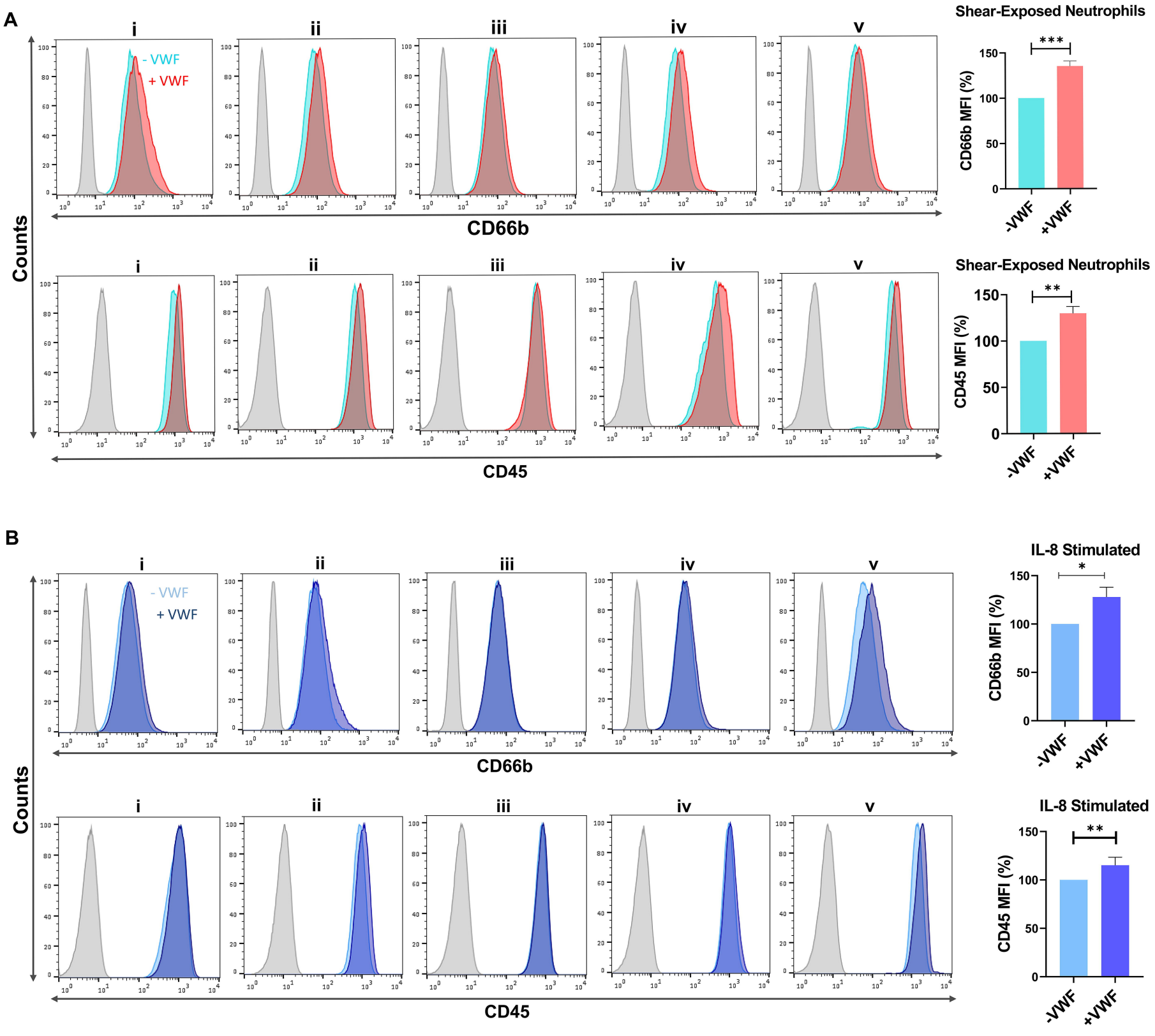
A
i
ii
iii
iv
v
- VWF
+ VWF
Counts
CD66b
CD45
Shear-Exposed Neutrophils
CD66b MFI (%)
CD45 MFI (%)
***
**
-VWF
+VWF
B
IL-8 Stimulated
*

Figure 7

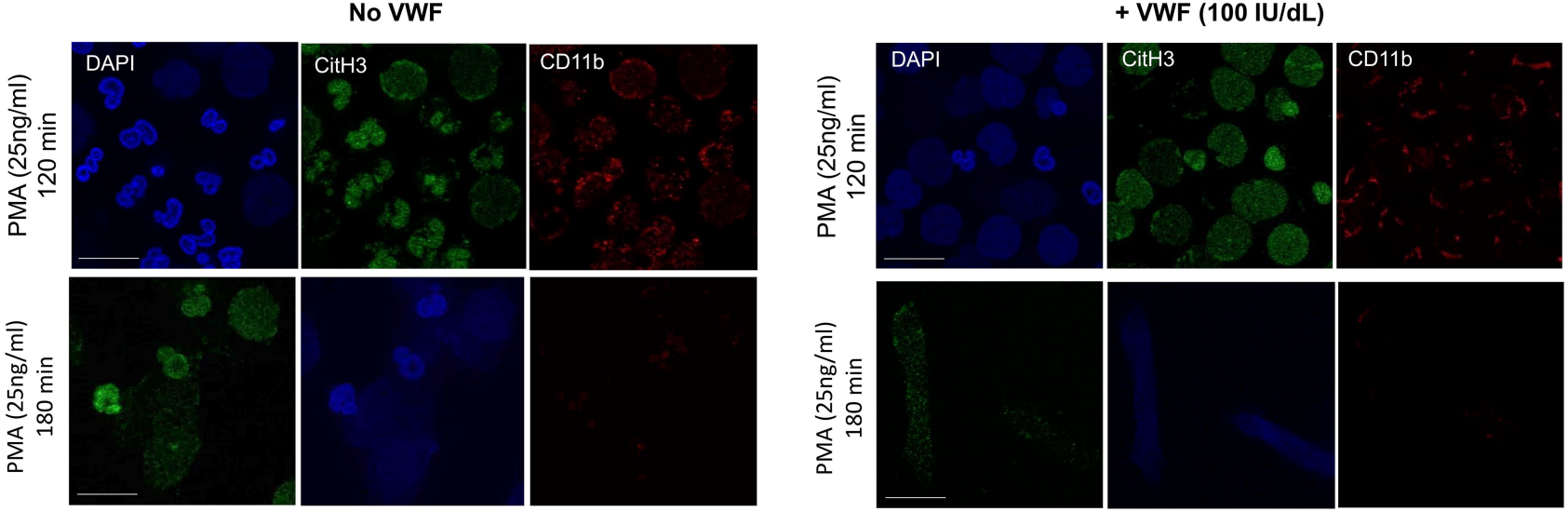
No VWF
+ VWF (100 IU/dL)
DAPI
CitH3
CD11b
PMA (25ng/ml)
120 min
PMA (25ng/ml)
180 min

Supplementary Data

Supplementary Methods

Isolation of human neutrophils from peripheral blood of healthy volunteers

Whole blood (5-10 ml) was collected from several healthy volunteers in EDTA tubes (Sarstedt, Germany) after obtaining informed consent, in compliance with the Declaration of Helsinki principles and the ethical guidelines of Germany. The volunteers had no history of impaired VWF or neutrophil function. They were healthy, infection-free, and had not taken any medications within 48 hours before blood collection. Neutrophils were isolated from peripheral blood immediately after collection using the EasySep™ Direct Human Neutrophil Isolation Kit (StemCell Technologies, Germany), according to the manufacturer's instructions. On average, 1.5-3 $X10^6$ cells /ml blood were isolated. The number and viability of isolated cells were determined using the NucleoCounter® NC-202™ (ChemoMetec, Denmark), a dual-color fluorescent automated cell counter that uses acridine orange (AO) and DAPI to identify live and dead cells. The purity of isolated cells was assessed by flow cytometry as described below.

We additionally determined cell viability and apoptosis after a incubation time of 180 minutes (min) using the Nucle-oCounter® NC-202™ and flow cytometry (by assessing CD16 receptor shedding), respectively.

Flow Cytometry

After isolation or incubation of neutrophils, cells were washed in PBS and resuspended in staining buffer (PBS containing 2% FBS and 2 mM EDTA). Cells were then immunostained with two panels of antibodies containing either fluorochrome-conjugated antibodies (anti-CD66b-FITC, anti-CD45-APC, and anti-CD16- PE) or isotype controls (IgG1-FITC, IgG1- APE, IgG1- PE). All antibodies were purchased from Miltenyi Biotec, Germany. After washing, cells were resuspended in a staining buffer and subjected to cytometric analysis using a Navios EX Flow Cytometer (Beckman Coulter, Germany). The attained data were further analyzed using FlowJo software (LLC, Becton Dickinson, USA).

Evaluation of VWF binding to neutrophils upon activation by inflammatory factors

After the isolation of neutrophils, cells suspended in autologous plasma (plasma obtained from the supernatant of the same isolated cells, containing plasma VWF) were transferred to multi-well plates. They were then either left untreated (resting cells) or stimulated with either 10 ng/ml PMA (Sigma, USA), 5 ng/ml TNFα (Invitrogen, Germany), or 0.3 ng/ml, 0.5 ng/ml, and 0.7 ng/ml IL -8 (R&D, USA) for 15 min at 37ºC, 5% CO_2.

To confirm if VWF interacts with neutrophils through the Mac-1 receptor on their surface, we conducted a series of experiments where isolated neutrophils were treated with Neutrophil Inhibitory Factor (NIF; R&D Systems, Germany) at a concentration of 400 ng/ml for 30 minutes at 37ºC with 5% CO2. As a control, another set of neutrophils was left untreated with NIF. Following this treatment, all neutrophils were stimulated with PMA (10 ng/ml) for 15 minutes at 37ºC with 5% CO2. Additionally, resting neutrophils (neither treated with NIF nor stimulated with PMA) were included in the experiments.

Cells were then washed with PBS and subjected to IF staining and microscopic analysis to quantify VWF signal intensity, as described below. At least three independent experiments were performed for each condition.

Evaluation of VWF binding to neutrophils upon exposure to shear forces

To assess the effect of shear flow on the binding of VWF to neutrophils, we performed experiments under static or flow conditions using the Bioflux 200 instrument (Fluxion Biosciences). We compared the VWF signal intensity between shear-exposed and resting cells through IF microscopy analysis. Initially, the isolated cells were centrifuged (300xg for 5 min) to remove the supernatant containing autologous VWF. They were then resuspended in RPMI medium (Roswell Park Memorial Institute medium 1640; Gibco, USA) containing glutamine and 10% FBS. A pdVWF/FVIII concentrate (Haemate from CSL Behring, Germany) either recombinant VWF (rVWF; VONVENDI from Baxalta, now part of Shire, Austria)was spiked to the cell suspension to achieve a final VWF antigen level of 100% (100 IU/dl). One fraction of the cells was incubated at 37ºC for 30 min under static conditions, while another fraction was exposed to a shear flow of 10 dyne/cm^2 for 30 min at 37ºC. To confirm the binding of the spiked pdVWF/FVIII or rVWF to neutrophils and exclude any potential VWF production induced by shear flow in neutrophils, we repeated the experiments by exposing the cells to shear flow in the absence or presence of pdVWF/FVIII or rVWF.

Subsequently, the cells were collected and fixed for subsequent IF staining analysis. At least three independent experiments were performed for each condition.

Investigation of VWF internalization by analysis of intracellular trafficking

To determine whether VWF is internalized by neutrophils, we visualized and examined VWF transport by studying the co-localization of VWF with early (EEA1) and late (Rab7) endosomal markers over time by IF microscopy analyses. In the first set of experiments, neutrophils were either fixed immediately after isolation or incubated (without any treatment) for 60 or 180 min and then fixed for subsequent immunostaining. In another series of experiments, we examined VWF trafficking upon interaction with neutrophils after exposure to shear stress for 30 min in the presence of pdVWF/FVIII, as described in the previous section. Afterwards, neutrophils were incubated for an additional 30 or 60 min at 37ºC and 5% CO_2 before fixing cells. The IF staining, microscopic image acquisition, and quantification of VWF/EEA1 and VWF/Rab7 co-localization were performed as described below.

The experiments were independently replicated at least twice, with each replication performed in triplicate (n=6).

Immunofluorescence microscopy analysis

The resting or treated cells were transferred to ibidi µ-Slide 4 wells (with glass bottoms and coated with poly-L-lysine; ibidi, Germany) at a concentration of 500,000 to 700,000 cells per chamber. Cells were then fixed with 10% formalin and permeabilized using a PBS-azide solution containing TritonX100. Primary antibodies used for immunostaining included rabbit polyclonal anti-human VWF (DAKO, Denmark), sheep polyclonal anti-human VWF (Abcam, UK), sheep anti-human FVIII (Haemato-logic Technologies, USA), mouse anti-human CD11b (Santa Cruz Biotechnology, USA), mouse anti-human EEA1 (BD Biosciences, USA), and mouse anti-human Rab7 (Santa Cruz Biotechnology, USA). The fluorescent secondary antibodies were anti-rabbit/ or anti-sheep Alexa Fluor-488, anti-mouse Alexa Fluor-555, and anti-mouse Alexa Fluor-633 nm (all available from Invitrogen, USA). A corresponding negative control was prepared for each experiment by excluding the primary antibodies. Imaging of cells was performed using an Apotome.2 microscope (Carl Zeiss, Germany). Three-dimensional (3D) images of stacked Z-series of images were created using the program ZEN 2.6 (blue edition; Carl Zeiss, Germany). VWF signals and VWF/EEA1

and VWF/Rab7 co-localization were quantified by measuring the mean VWF intensity value (MIV) and Pearson correlation coefficients, respectively, for at least n = 25 cells (for internalization experiments under static conditions) or n=50 (for internalization experiments under shear flow, as well as measuring MIV) of the stacked Z images using the program ZEN 2.6.

Measurement of VWF content in the supernatant of neutrophils

To further confirm the internalization of VWF by neutrophils, we measured VWF antigen (VWF:Ag) in supernatants from resting and stimulated neutrophils and compared the amount of VWF with the amount in supernatants without cells (as a negative control). After neutrophils were isolated from whole blood (n=6), cell suspensions were centrifuged (300xg for 5 min), and supernatants containing autologous VWF were collected in new tubes. Cell pellets were then resuspended in the same autologous supernatant at a cell concentration of 6 $X10^6$ cells/1 ml. Cells were left untreated or stimulated with IL -8 (0.7 ng/ml), PMA (10 ng/ml), or TNFα (5 ng/ml) for 15 min at 37ºC. Cell supernatants were then collected after centrifugation (350 g for 5 min), and VWF:Ag levels were measured, as previously described, in cell supernatants and supernatants deprived of neutrophils.[15]

Purification of pdVWF/FVIII concentrates

The pdVWF/FVIII concentrate (Haemate, CSL Behring, Germany) was purified to eliminate potential impurities present in the Haemate concentrate (e.g., albumin), for use in experiments assessing the effect of plasma on neutrophil characteristics. The purification was performed by size-exclusion chromatography on the ÄKTA pure 25 system (Cytiva/GE Healthcare Life Sciences, USA) using a Superdex 200 Increase 10/300 GL column (Cytiva, Germany).The protein purity and presence of VWF in the fractions corresponded to the VWF peak were confirmed using SDS-PAGE gel analysis.

Western blotting and gel electrophoresis of neutrophil lysates

Neutrophils were either left untreated or stimulated with IL -8 (0.7 ng/ml; for 15 min at 37ºC) in the presence of autologous VWF. Subsequently, washed cells were either directly proceeded to cell lysis or first suspended in RPMI buffer and incubated for 60 or 180 min at 37ºC and 5% CO_2 before cell lysis. Cell lysis was performed in M-PER

reagent® (Thermo Scientific, USA) supplemented with a protease inhibitor cocktail tablet (Roch, Germany) according to the manufacturer's instructions. Western blotting of neutrophil lysate together with the lysates of cells producing VWF as controls (including healthy individual-derived ECFCs producing endogenous VWF and transfected HEK293T cells producing recombinant VWF) were performed using 4-15% Mini-Protean® TGX and Mini Trans-Blot® Cell systems under reducing condition (Biorad, USA), according to the manufacturer's guidelines. After blotting, VWF was visualized with rabbit polyclonal antibodies against human VWF (Dako, Denmark) and antibodies against rabbit IgG conjugated to horseradish peroxidase (Biorad, USA), as described elsewhere.[16]

To determine whether the VWF detected in the neutrophil lysate from the WB experiment was taken up from outside the cell, the purified pdVWF/FVIII (Haemate-P®) was fluorescently labeled using the FluoReporter™ FITC protein labeling kit (Invitrogen, USA) according to the producer's instructions. Neutrophils were then stimulated with IL -8 (0.7 ng/ml; for 15 min at 37ºC) in the presence of the fluorescently labeled VWF (at a VWF antigen concentration of 100 IU/dL), incubated, and lysed, as described above. To assess the integrity of pdVWF/FVIII after exposure to the stimulated neutrophils, cell lysates were subjected to gel electrophoresis on 4-15% Mini-Protean® TGX (Biorad, USA) at 180 V for 60 min under reducing condition. The fluorescence signal was detected using the ChemiDocTM MP imaging system (Biorad, Germany).

Investigation of the effects of VWF on the expression of neutrophils chaqracteristics

To evaluate impact of VWF binding on expression of neutrophice surface proteins, isolated, washed neutrophils (n=5 healthy individuals) were resuspended in RPMI medium (containing glutamine and 10% FBS) and stimulated either with IL -8 (0.7 ng/ml; for 15 min at 37ºC) or by shear forces (10 dyne/cm^2 generated by the Bioflux 200). Experiments were performed without or with the purified pdVWF/FVIII concentrate (Haemate, CSL Behring, Germany). Cells were then subjected to flow cytometric analysis described above to determine the surface expression of CD16, CD45, and CD66b proteins.

Further, we evaluated the impact of VWF on the formation of Neutrophil Extracellular Traps (NETs). Isolated neutrophils, in the presence or absence of pdVWF (at a VWF

antigen concentration of 100 IU/dL), were stimulated with PMA (25 ng/ml) at 37°C with 5% CO2 for different time points: 60, 120, 180, and 240 minutes. The cells were then fixed and subjected to immunofluorescence (IF) staining. The staining of the chromatin was done by using DAPI and Cit-Histone H3 antibody (ThermoFisher, Germany). The experiments were independently replicated at least twice, with each replication performed in duplicate (n=4).

Statistical analysis

The statistical significance of differences in data was evaluated with the unpaired Student's test using GraphPad Prism version 8.0.1 (GraphPadSoftware). Figures are presented as mean ± SEM. A p-value ≤.05 was considered to be statistically significant.